Minimizing the total annualized cost of "SIDEM" seawater desalination unit

Maha Ben Hamad[a],*, Rubén Ruiz-Femenia[b], Ali Snoussi[a], Ammar Ben Brahim[a], José A. Caballero[b]

[a]*Research Unit of Applied Thermodynamics (UR11ES80), National Engineering School of Gabes, University of Gabes, Omar Ibn El Khattab St, 6029 Gabes, Tunisia, email: benhamadmaha@yahoo.fr (M.B. Hamad), ali.snoussi38@gmail.com (A. Snoussi), ammar.benbrahim@enig.rnu.tn (A.B. Brahim)*
[b]*Department of Chemical Engineering, University of Alicante, Ap. Correos 99, 03080 Alicante, Spain, email: ruben.ruiz.fe@gmail.com (R. Ruiz-Femenia), caballer@ua.es (J.A. Caballero)*

ABSTRACT

This paper presents a steady state analysis of a multi-effect thermal vapor compression desalination plant (MED-TVC) installed in the Tunisian Chemical Group (GCT) factory. A thermodynamic model includes mass and energy balances of the system are presented. An economic model is developed to estimate the cost of produced water ($/m³). The proposed models to minimize the total annualized cost (TAC) of the desalination unit are based on a combination between the process simulator Aspen HYSYS and Matlab. The effects of the operating parameters variations on the system's performance were studied. The simulation results show a good agreement with the industrial data of the pilot unit.

Keywords: Steady state; Multi-effect; Thermal vapor compression; Desalination; Optimization

1. Introduction

In the recent years the demand of pure water increases caused to the rapid population growth and the evolution of industrial applications. The International Desalination Association [1] reports that currently there are more than 18,000 desalination plants in operation worldwide, with a maximum production capacity of around 90 million m³/d of fresh water [1]. Desalination technologies can be divided in two categories: thermal and membranes systems. The process of multi-effect distillation coupled with thermal vapor compressor (MED-TVC) is one of the most important thermal desalination units.

El-Dessouky and Ettouney [2] presented detailed mathematical and economic analysis for the thermal desalination plants (multi-stage flash (MSF), multi-effect distillation (MED), multi-effect thermal vapor compression (MED-TVC) and multi-effect mechanical vapor compression (MED-MVC)). In literature, many studies [3–5] have been published about the applications of the first and the second laws of thermodynamics to analyze the MED-TVC systems. The models were based on mass, energy and exergy balances equations and the thermodynamics properties of seawater.

The application of numerical simulation approach to study and optimize the MED-TVC and MSF desalination units presented in several papers as in [6–9]. In these works, authors presented several steady state and dynamics models using different software such as Aspen Custom Modeler, computational flow dynamics (CFD), gPROMS simulator and discussed their simplicity and flexibility in order to modify inputs parameters, model correlations or process equipment as well as the economic evaluation.

Due to the development of thermal desalination technologies, recent researches focused on the optimization and parametric study of these plants. Several studies

*Corresponding author.

[10–12] investigated in the effect of operating conditions (i.e flow rate and temperature of feed seawater, steam temperature) and in the design conditions such as; number of effects, the scale thickness of the first effect and the condenser. They studied their influences on the production rate and the gain output ratio (GOR) value on different industrial MED (with and without TVC) units and their simulation results were compared with models from literature. Kouhikamali et al. [13,14] studied the effect of the pressure drop of condensation inside tubes and evaporation outside tubes in the heat exchanger on the energy consumption. The influence of the length and diameter of tubes on the plant performance and the system costs were investigated. A work by Al-Mutaz et al. [15] describe the influence of changing the suction position of the thermal vapor compressor as well as the effect of suction pressure on the energy consumption and the specific heat transfer area of a MED-TVC plant.

An important works by Dahdah and Mitsos [16,17] present various new configurations combine thermal desalination with thermal compression systems. Authors focused on the location of a steam ejector to find the optimal design of hybrid MED-TVC-MSF system. Further, a multi-objective structural optimization is performed in which the GOR of the structures is maximized while the specific heat transfers area requirements (sA) are minimized using the General Algebraic Modeling System (GAMS) as the solver of the problem. On the other hand, Skiborowski et al. [18] optimized a superstructure of a reverse osmosis (RO) and a forward-feed MED hybrid system. They presented an optimization strategy using a non-linear program to obtain the optimal configuration.

Under the increasing price of oil and the high energy consumption of thermal plants, several researches [19,20] have been published on the thermo-economic optimizations of these systems. In literature, fewer studies are carried out on the multi-objective optimization (MOO) in order to minimize the total annualized cost (TAC) of desalination systems. Tanvir et al. [21] suggested a combination between gPROMS model and optimization routines to minimize the TAC of MSF plant. Druetta et al. [22] developed a nonlinear problem to determine the nominal optimal sizing of equipment and optimal operating conditions that satisfy a fixed nominal production of fresh water at minimum TAC for a MED unit. In this research, the equations were implemented in GAMS (General Solver Modeling System) and CONOPT was used as a NLP local solver. Esfahani et al. [23] proposed a MOO to minimize the TAC, maximize the GOR and the product water flow rate for a MED-TVC system based on exergy analysis by using a genetic algorithm (GA).

In literature, published papers presented two ways to study and solve the different problems approaches for the MED-TVC systems; programming algorithms or several commercials process simulators. In contrast, this paper presents a new method to minimize the TAC of MED-TVC plant based on a combination between Matlab and the process simulator Aspen HYSYS. The mathematical and economic equations defining the unit are implemented in Matlab and the flowsheet of the unit is created with Aspen HYSYS. This approach can be applied in several problems such as the process design, the parametric study and the economic analysis.

The paper is organized as follows: Section 2 presents a brief description of the MED-TVC desalination unit. Sections 3 and 4 describe the assumptions used to simplify the study, the mathematical and the economic models used to obtain the cost of produced water (in $/m³). The problem formulation and the proposed simulation-optimization are illustrated in section 5 with the decision variables and constraints. Section 6 then combines the results of simulations and a parametric study of several parameters. The last section is devoted to concluding remarks.

2. MED-TVC process description

The desalination plant presented in this paper is an actual MED-TVC unit located in the phosphoric acid plant owned by the GCT in the industrial area of Gabes (south of Tunisia). The GCT investigated in the thermal plants with different capacities in their industrials factories. The choice of this type of plant has many reasons: the need of pure water used in the production of phosphate and its derivatives, the availability of heating steam produced by the turbine and the factories locations near the sea.

The presented unit manufactured by the French Company "SIDEM". It composed by three evaporators, a thermal vapor compressor and a condenser. A schematic of the SIDEM unit is shown in Fig. 1. The seawater enters in the tubes of down condenser (after treatment), its temperature increases a few degrees due to the condensation of an amount of steam, comes from the last effect, in the shell side. Then, the seawater flow rate is divided into two parts; the first part rejected to the sea called cooling water and the second is distributed equally between the effects. Thermal vapor compressor is used to compress the motive steam from the external source and entrain a part of vapor produced in the last effect. The compressed stream (V_{cv}) enters in the tubes of the first effect. In each effect, the heat steam enters in the tubes and the feed seawater is sprayed with the nozzles located in the summit of the effect. Steam condenses inside into distillate which heats the feed seawater outside the tubes. Part of seawater evaporates and generates an amount of vapor, which passes to the tubes of the next effect as a heat source. The second part represents the rejected brine. This process is repeated for all effects. Brine and distillate are collected from effect to effect until the last one and finally are extracted by centrifugal pumps.

3. Assumptions and mathematical model

3.1. Assumptions

In order to obtain a simple mathematical model, the following assumptions are considered:

- The desalination plant operates in steady state [19].
- Thermodynamics losses include just the boiling point elevation (BPE) [15].
- Pressure drops across the demister and during the condensation are neglected [22].
- The dimensions of each equipment; effects, compressor, condenser (length, width and height) are not included in the model [22].
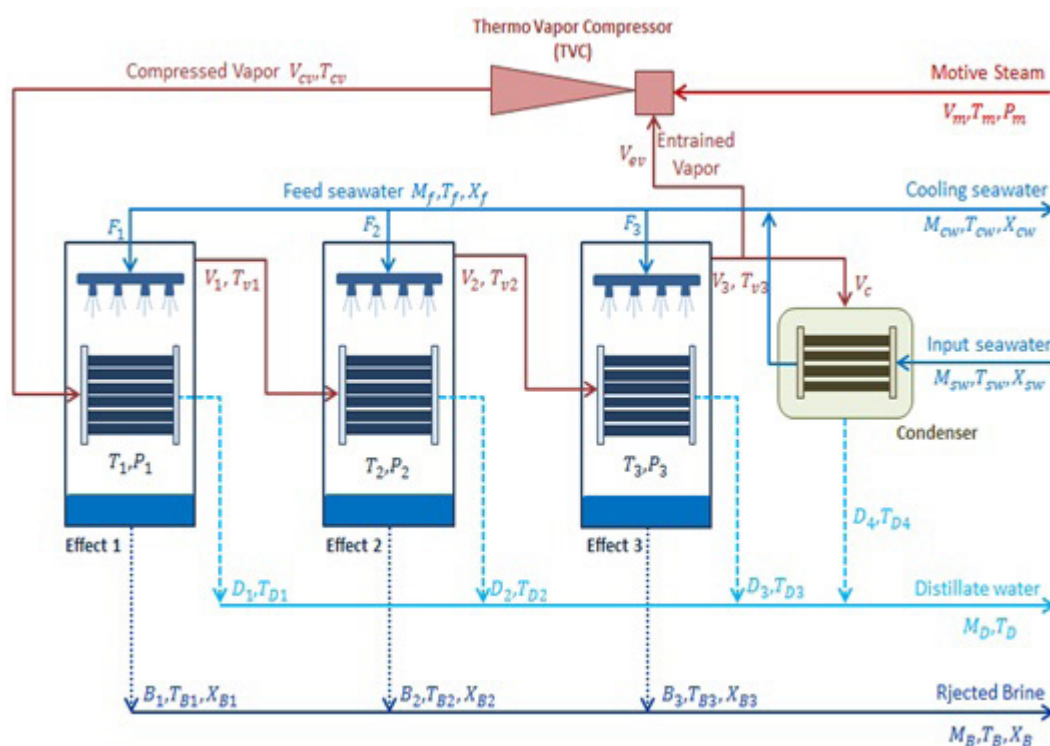
Fig. 1. Flow diagram of MED-TVC system (SIDEM unit).

- The distillate water and vapor formed in effect are free of salt [23,24].
- Heat losses from desalination to the surroundings are negligible because the system operates at low temperature (between 100 and 40°C [24]).
- Physical properties of seawater are taken as a function of temperature and salinity [2].
- To achieve the optimum operating conditions, temperature difference between all effects is assumed to be equal. T_1 and T_n are the first and the last effect temperature respectively, the temperature difference can be expressed as [5,25]:

$$\Delta T = \frac{T_1 - T_n}{n-1} \tag{1}$$

$$T_1 = T_{cv} - \Delta T \tag{2}$$

$$T_{i+1} = T_i - \Delta T , \quad i = 2\ldots n \tag{3}$$

3.2. Mathematical model

As mentioned earlier, Fig. 1 shows a schematic diagram of the system with the configurations of streams. Fig. 2 shows the inlet and outlet streams of an effect of the desalination unit. The mathematical model based on the mass balances, the energy balances, the salt mass conservation law and the heat transfer equations. The model also includes correlations for estimating the heat transfer coefficients, thermodynamics losses and the physical properties of seawater.

In an effect i, the brine temperature T_{bi} is assumed to be equal to the effect temperature T_i while the vapor temperature T_{vi} can be calculated as follows:

$$T_{vi} = T_i - BPE \tag{4}$$

where the boiling point elevation BPE is the increase in the boiling temperature due to the salts dissolved in the water, calculated with the correlation given in Appendix.

The feed seawater M_f is distributed equally to all effects with mass flow rate F_i, which can be calculated as follows:

$$F_i = \frac{M_f}{n} \tag{5}$$

where n is the number of effects in the desalination system. The mass balances in the first and in each effect can be calculated by:

$$F_1 = V_{cv} + B_1 \tag{6}$$

$$F_i = V_i + B_i \tag{7}$$

Salt balance in the first and each effect can be written as:

$$X_{f1}F_1 = X_{b1}B_1 \tag{8}$$

$$X_{fi}F_i = X_{bi}B_i \tag{9}$$

Energy balance in the first and each effect is expressed as follows:

$$V_{cv}\lambda_{cv} = F_1C_{p1}\left(T_1 - T_f\right) + V_1\lambda_1 \tag{10}$$
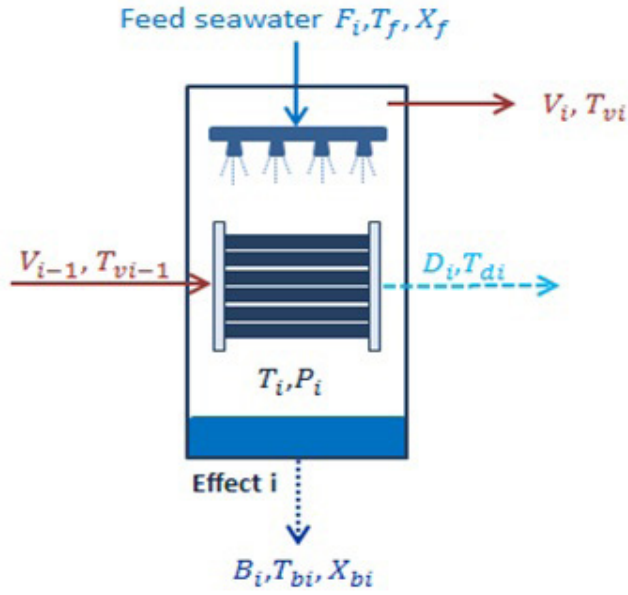
Fig. 2. Scheme and model variables for the i-th effect.

$$V_{i-1}\lambda_{i-1} = F_i C_{pi}\left(T_i - T_f\right) + V_i\lambda_i \tag{11}$$

In which C_{pi} is the specific heat capacity for seawater. λ_i and λ_{cv} are the latent heat of vaporization at the effect temperature and at the compressed vapor temperature, respectively. These parameters are calculated using the correlations given in the Appendix.

The heat flows in the first and each effect were:

$$Q_{e1} = V_{cv}\lambda_{cv} \tag{12}$$

$$Q_{ei} = V_i\lambda_i \tag{13}$$

Therefore, the heat transfer area of the ith effect and the total heat transfer area can be obtained as follows:

$$A_{ei} = \frac{Q_{ei}}{U_{ei}(LMTD)_i} \tag{14}$$

$$A_t = \sum_{i=1}^{n} A_{ei} \tag{15}$$

The logarithmic mean temperature difference $(LMTD)_i$ and the overall heat transfer coefficient U_{ei} is estimated using the correlations presented by El-Dessouky et al. [2].

$$(LMTD)_i = \frac{(T_i - T_f)}{\ln\left(\frac{T_{v_{i-1}} - T_f}{T_{v_{i-1}} - T_i}\right)} \tag{16}$$

$$U_{ei} = 1.9394 + 1.40562 \times 10^{-3} T_{bi} - 2.07525 \times 10^{-5}\left(T_{bi}\right)^2 \\ + 2.3186 \times 10^{-6}\left(T_{bi}\right)^3 \tag{17}$$

Similarly, the energy balance and the heat transfer area of the condenser can be written as follows:

$$V_c\lambda_n = \left(M_f + M_{cw}\right)C_p\left(T_f - T_{sw}\right) \tag{18}$$

$$A_{con} = \frac{V_c\lambda_n}{U_{con}(LMTD)_{con}} \tag{19}$$

The logarithmic mean temperature difference LMTD and the overall heat transfer coefficient can be calculated using the following equations [2]:

$$(LMTD)_{con} = \frac{\left(T_{vn} - T_{sw}\right) - \left(T_{vn} - T_f\right)}{\ln\left(\frac{T_{vn} - T_{sw}}{T_{vn} - T_f}\right)} \tag{20}$$

$$U_{con} = 1.7194 + 3.2063 \times 10^{-2}\left(T_{vn}\right) + 1.5971 \times 10^{-5}\left(T_{vn}\right)^2 \\ + 1.9918 \times 10^{-7}\left(T_{vn}\right)^3 \tag{21}$$

where T_{vn} is the vapor temperature of last effect.

The energy balance of the compressor is used to calculate the enthalpy of the compressed vapor h_{cv} as follows:

$$V_m h_m + V_{ev} h_{ev} = \left(V_m + V_{ev}\right)h_{cv} \tag{22}$$

$$h_{cv} = \left(\frac{\frac{V_m}{V_{ev}}h_m + h_{ev}}{1 + \frac{V_m}{V_{ev}}}\right) \tag{23}$$

where h_m and h_{ev} are the specific enthalpy of the motive steam and the entrained vapor, respectively, both estimated with correlations presented in the Appendix.

On other hand, the entrainment ratio (Ra) is an essential parameter to evaluate the performance of compressor. It can be determined by several methods available in the literature [17,25]. El-Dessouky and Ettouney [2] presented in a semi-empirical model to calculate the entrainment ratio as follows:

$$Ra = 0.296 \frac{\left(P_{cv}\right)^{1.19}}{\left(P_{ev}\right)^{1.04}}\left(\frac{P_m}{P_{ev}}\right)^{0.015}\left(\frac{PCF}{TCF}\right) \tag{24}$$

where P_{cv}, P_{ev} and P_m refer to the pressures of compressed vapor, entrained vapor and the motive steam, respectively. PCF and TCF [2] are two correction factors and can be calculated by Eqs. (25) and (26). These equations are valid for $10°C \le T_{ev} \le 500°C$, $100kPa \le P_m \le 3500kPa$, $1.81 \le CR = \dfrac{P_{cv}}{P_{ev}} \le 6$ and $Ra \le 4$.

$$PCF = 3 \times 10^{-7}\left(P_m\right)^2 - 0.0009\left(P_m\right) + 1.6101 \tag{25}$$

$$TCF = 2 \times 10^{-8}\left(T_{ev}\right)^2 - 0.0006\left(T_{ev}\right) + 1.0047 \tag{26}$$

3.3. Performance parameters

The following parameters are used to analyze the performance of MED-TVC systems [2]:

- The gain output ratio (GOR) is defined as the ratio between the distillate produced water and the motive steam.

- The specific cooling water flow rate (sM_{cw}) is defined as the ratio between the flow rate of produced water and the cooling seawater.
- The specific heat transfer area (sA), which is the ratio between the sum of the heating surface area of equipment (effects and condenser) and the flow rate of product water.

In the thermal desalination units, a specific characteristic related to the first law of thermodynamic, which is defined as the thermal energy consumed by the system to produce 1 kg of distilled water calculated as [4]:

$$sQ = \frac{V_m \lambda_m}{M_d} \tag{27}$$

According to the second law of thermodynamic, the specific exergy (S_{ex}), can be introduced to evaluate the performance of the MED-TVC system. It is defined as the exergy consumed by the motive steam to produce 1 kg of distillate water when the steam and the liquid assumed to be saturated at ambient temperature T_0, is calculated as follows [23]:

$$S_{ex} = \frac{V_m}{M_D}\left[\left(h_m - h_{fd}\right) - T_0\left(S_m - S_{fd}\right)\right] \tag{28}$$

where S_m is the specific entropy of inlet motive steam, h_{fd} and S_{fd} are, respectively, the specific enthalpy and entropy of outlet condensate at saturated liquid. These parameters are calculated using correlations in the Appendix.

4. Economic model

The unit product cost for desalination plants depends on many factors as: the capacity, size, type of technology applied and plant location [27,28]. Generally, the units with small size (≤5000 m³/d) exhibit the highest costs, whereas the larger plant capacity reduces the cost for unit product. For the MSF units, which have a daily capacity of 23,000–528,000 m³, the costs of the produced water ranges between 0.52–1.75 $/m³. For smaller MED and MED-MVC units (less than 500 m³/d), their unit product costs is in the range of 2.5 and 10 $/m³. The costs of existing commercial MED-TVC plants installed in many countries are higher compared with the others capacities for the same desalination technology; in which their unit product cost ranges between 0.5–5.4 $/m³ [29,30]. Fig. 3 shows the unit product cost of some existing MED-TVC systems around the world over their total capacity [30].

In this work, the total annualized cost (TAC) of the SIDEM plant defined as the sum of the capital costs of equipment (CAPEX) and the operational expenses (OPEX) [31].

$$TAC = CAPEX + OPEX \tag{29}$$

The total capital costs CAPEX accounts the costs of effects evaporator, the condenser and the thermo-compressor. The capital costs of pumps, mixer and splitter are not included in this model. In order to simplify the economic equations, the effects assumed to be one evaporator with total heat transfer are A_t. The total capital expenditures are given by the following equation [31]:
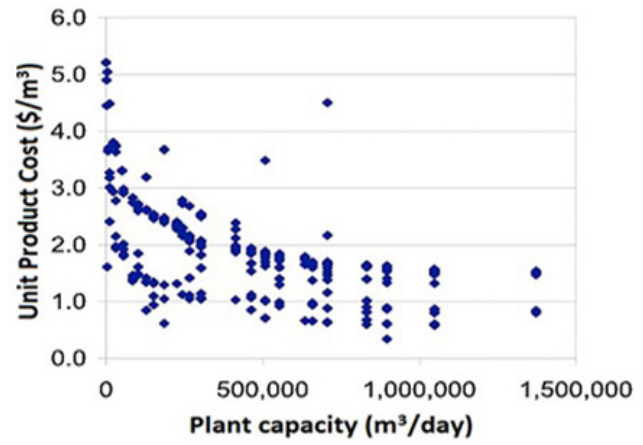
Fig. 3. Unit produced costs of commercial MED-TVC systems [30].

$$CAPEX = a_f\left(\frac{CEPCI_{2015}}{CEPCI_{2001}}\right)\left((C_p^0 F_{BM})_{evaporator} + (C_p^0 F_{BM})_{condenser} + (C_p^0 F_{BM})_{compressor}\right) \tag{30}$$

where a_f represent the amortization factor which is given by the following equation:

$$a_f = \frac{i_r(i_r + 1)^y}{(i_r + 1)^y - 1} \tag{31}$$

where i_r refers to the interest rate per year and y is the number of years.

In Eq. (30), C_p^0 indicates the basic cost of a unitary equipment (in US$) operating at pressure close to ambient conditions. F_{BM} corresponds to the correction factor for the unitary equipment cost, in which the materials of construction and the operational pressure of the equipment are correlated [28,32].

The basic unitary cost of the condenser is estimated using the correlations proposed by Turton et al. [28] which depends on the heat transfer area and the pressure of condenser. To estimate the unitary cost of the evaporator and compressor, the Couper et al.'s correlations [32] are used in the model. These correlations depend on the heat transfer area for the evaporator and for the thermal vapor compressor depend on the mass flow rate and the pressure of the entrained vapor.

In addition, in Eq. (30), the costs should be corrected with the Chemical Engineering Plant Cost Index (CEPCI).

Operational expenditures account the steam consumed by the thermo-vapor compressor and expressed as:

$$OPEX = C_{steam}Q_s \tag{32}$$

where C_{steam} is the specific steam cost giving by the GCT factory data. The term Q_s indicates the annual steam consumption.

Finally, the cost of produced water per m³ can be written as:

$$C_{porduction}\left(\$/m^3\right) = \frac{TAC\left(\$/year\right)}{3600 \times 24 \times 350 \times Q_p\left(m^3/s\right)} \tag{33}$$

where Q_p is the volumetric flow rate of produced water.

5. Problem formulation

The objective function is to minimize the total annualized cost (TAC) of the desalination process. The purpose of this paper is to use a combination between Matlab as a process optimizer and Aspen HYSYS as a process simulator to solve the problem.

Matlab R2013a is used to implement the equations model. The function '*fmincon*' used to find the minimum TAC [33,34] from several equations based on vector of variables between minimum and maximum values and under defined constraints. The Sequential Quadratic Programming (SQP) algorithm has been chosen as a method to solve the non-linear problem based on successive iterations to find the feasible solutions [34,35].

The desalination unit is modeled using Aspen HYSYS V8.4 for a steady state simulation. Due to the specific characteristics of seawater, NRTL-electrolyte fluid package was chosen in this study to calculate equilibrium and thermodynamics properties [13]. The flowsheet in Aspen HYSYS is shown in Fig. 4.

The connection between Matlab and Aspen HYSYS is done via the Component Objective Model (COM) interface of Microsoft with ActiveX technology [34]. The initial values are provided in Matlab in which transfers the parameters to Aspen HYSYS. Then, Aspen HYSYS is employed to simulate the desalination system through the flowsheet. Aspen HYSYS returns the simulations results to Matlab; the TAC is calculated and the constraints function is verified. This iterative process is carried out until the convergence criteria are satisfied and the final results are obtained [36–38]. The flow diagram of the connection between Aspen HYSYS and Matlab is shown in Fig. 5.

The selected decisions variables in this work are: mass flow rate and pressure of the motive steam, temperature of feed sea water to effects, pressure of the last effect and the pressure of the compressed vapor pressure (output of TVC). Furthermore, the linear and nonlinear constraints of the problem are introduced below.

To avoid temperature crosses among effects, the following conditions must be satisfied:

$$T_i > T_{i+1} \tag{34}$$

$$\Delta T = 10°C \tag{35}$$

During the simulation no pressure drop in the intercooler and the effect pressure should be decrease from an effect to other in which streams pressures are limited by:

$$P_i > P_{i+1} \tag{36}$$

For environmental limited the salt concentration of the rejected brine is limited with upper value as follow:

$$X_B \leq 70,000 \ ppm \tag{37}$$

6. Case study and results

6.1. Case study

The parameters used in this study of the SIDEM unit presented by the Phosphoric Acid Plant owned by the GCT factory installed in Gabes (south of Tunisia) and shown in
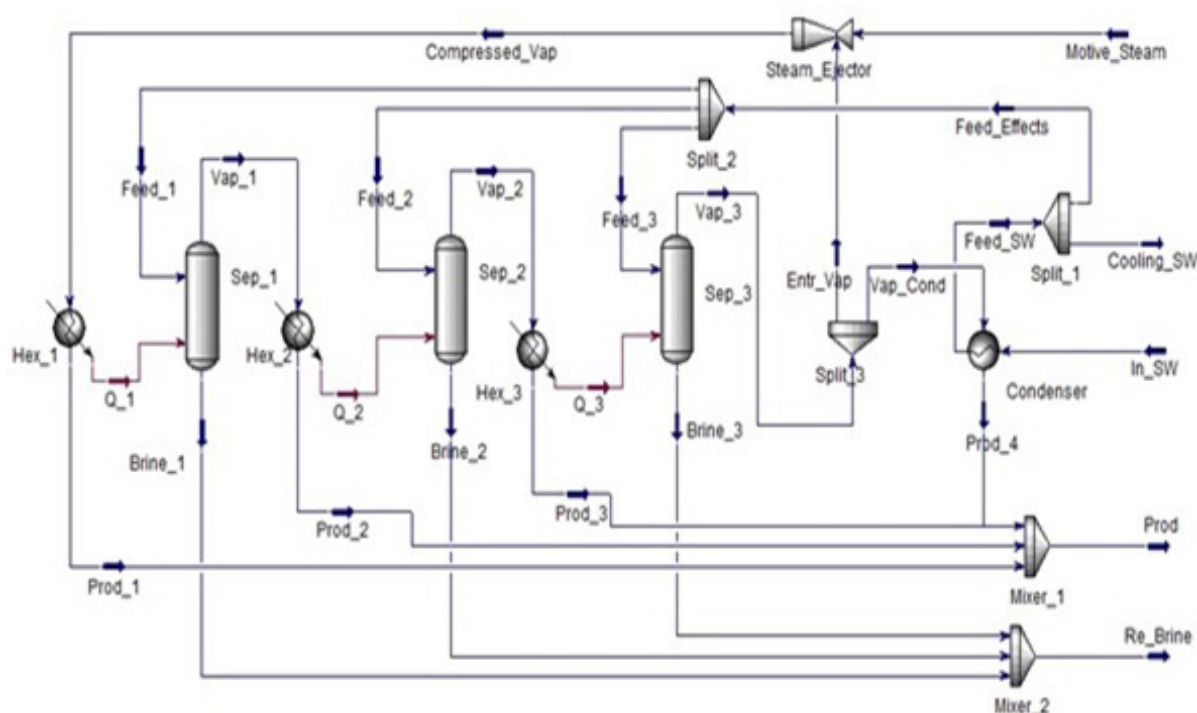
Fig. 4. Aspen HYSYS flowsheet for SIDEM unit.
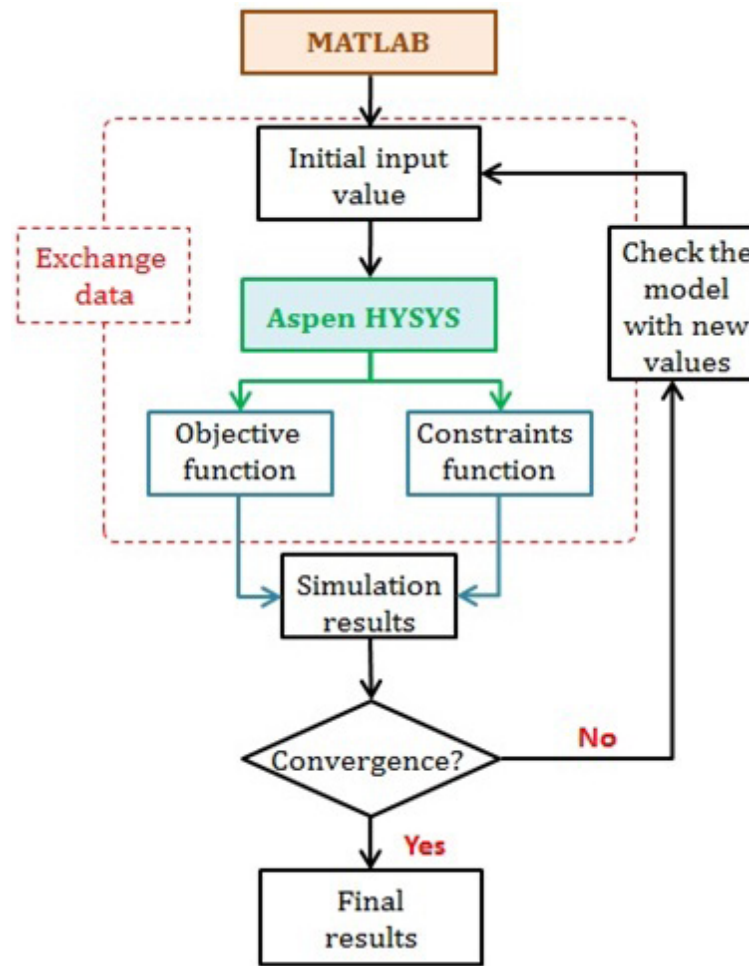
Fig. 5. Flowchart of the proposed combination.

Table 1. Table 2 summarizes the required parameters for the economic model.

6.2. Simulation results

The proposed model presented in the paper is validated with results from the GCT factory. The comparison between the calculated results by the model and the industrial data, as mentioned in Table 3, shows an accuracy of ±10%.The total distillate capacity of the system is 22.87 t/h while the feed seawater flow rate to effects is 60 t/h. In addition, 1.5 ton/h of vapor condensate in the condenser and causes the increase of the input seawater temperature around 4°C. On other hand, the salinity of rejected brine is 58,300 ppm with temperature about 40°C, which is lower than the limited value indicated the constraints. This value cannot be supplied by the factory.

The feed seawater is distributed equally between all effects with mass flow rate 20 t/h and temperature 32°C. The simulated results for the three effects of SIDEM unit are presented in Table 4. The decrease of effect temperature leads to reduction in the energy consumption and the overall heat transfer coefficients. The heat input to each effect is required to produce from the feed seawater. It should be highlighted that in

Table 1
The operating parameters

Parameter (unit)		Value
Seawater	Mass flow rate (t/h)	220
	Temperature (°C)	28
	Pressure (bar)	3
	Salinity (ppm)	39,000
Motive steam	Mass flow rate (t/h)	3
	Temperature (°C)	170
	Pressure (bar)	5
Condenser	Pressure drop tube (bar)	0.3
	Pressure drop shell (bar)	0
	Temperature drop (°C)	4
Ejector	Pressure output (bar)	0.25
effects	Temperature 1 (°C)	60
	Temperature 2 (°C)	50
	Temperature 3 (°C)	40
Cooling seawater	Mass flow rate (t/h)	160
Feed to effects	Mass flow rate (t/h)	20

all effects, approximately, 30% of mass flow rate of seawater evaporate and the average BPE losses alone are 0.8°C.

Fig. 6 shows a comparison between the simulations results and the industrial values of the pressure inside the three effects of SIEDM unit. Good agreement was found between the simulations results and the actual data from the factory. The pressure effects decrease from 0.1955 bar in the first effect to 0.07248 bar in the last effect.

The simulation results of the thermo-vapor compressor and the industrial data are listed in Table 5. The motive steam entrained 4.946 t/h of vapor from the last effect with a pressure of 0.07248 bar. The compressor of the SIDEM unit has a higher CR value (around 3.42) compared to other units in literature [2–4]. As shown by Table 5, the pressures values deviations between the actual data and the simulations results induce the change of the CR value.

The performance parameters of the SIDEM plant are illustrated in Table 6. The specific heat transfer area As obtained by this simulation is 96.79, which is very low compared to the literature [4–11]. On the other hand, the overall heat transfer coefficients in all effect is in the average of 2.4 kW/(m² °C). Any change in the temperatures leads to
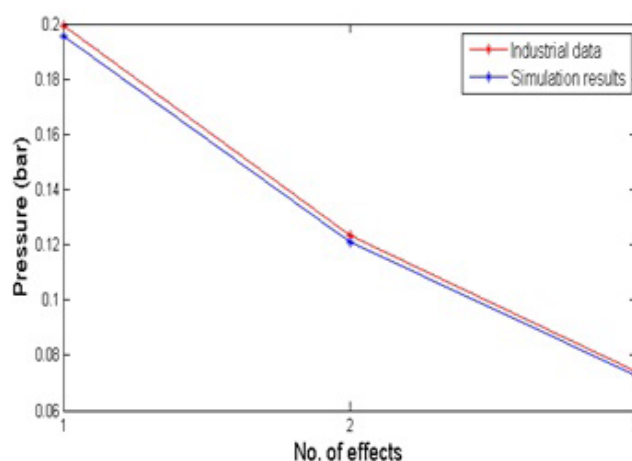
Fig. 6. Comparison of simulation results and actual data of pressure effects.

Table 2
Economic parameters

Parameters	Value
Cost of Steam C_{steam}, $/ton	16.61
Amortization year y, year	10
Interest rate i, %	10
Annual operating hours	24×350

Table 3
Comparison of simulation results and industrial plant data

Parameters (unit)	Calculated	Actual	Deviation (%)
Total distillated produced water M_D (t/h)	22.8704	21.67	+5.54%
Temperature of produced water T_D (°C)	39.65	NA[a]	–
Seawater temperature T_{sw} (°C)	28	28	–
Number of effects	3	3	–
Feed seawater temperature T_f (°C)	32	32	–
Total rejected brine flow rate M_B (t/h)	40.1256	41.33	–2.9%
Salinity of rejected brine X_B (ppm)	58,300	NA[a]	–
Temperature of rejected brine T_B (°C)	40.01	NA[a]	–
Vapor enter to condenser V_c (t/h)	1.5048	NA[a]	–
Pressure of last effect P_3 (bar)	0.07248	0.074	–2.054%
Cooling seawater M_{cw} (t/h)	160	160	–

[a]: Not Available

Table 4
Results of simulation

Parameter (unit)	Effect 1	Effect 2	Effect 3
Temperature T_i (°C)	60	50	40
Produced water mass flow rate D_i (t/h)	7.9452	7.056	6.3684
Produced vapor mass flow rate V_i (t/h)	7.056	6.3684	6.4512
Temperature of produced vapor T_{vi} (°C)	59.2241	49.2561	39.2870
Outline brine flow rate B_i (ton/h)	12.9456	13.6332	13.5504
Overall heat transfer coefficients U_{ei} (kW/m²°C)	2.4498	2.2476	2.1108
Heat flow Q_{ei} (kW)	5267	4631	4501
Heattransfer area (m²)	97.4735	246.5064	234.4532

Table 5
Results of simulation of the thermal vapor compressor

Parameters (unit)	Calculated	Actual	Deviation (%)
Entrained vapor flow rate V_{ev} (t/h)	4.9464	4.55	+8.712%
Temperature of compressed vapor T_{cv} (°C)	84.5	90	−6.11%
Pressure of entrained vapor P_{ev} (bar)	0.07248	0.074	−2.054%
Pressure of compressed vapor P_{cv} (bar)	0.248	0.25	−0.8%
Compression ratio CR	3.42	3.39	−0.8%
The entrainment ratio Ra	2.31	–	–
Specific enthalpy of compressed vapor H_{cv} (kJ/kg)	2650.6	NA[a]	–

Table 6
System performance

Parameter (unit)	Model
Specific cooling water flow rate sM_{cw}	0.1429
Specific heat transfer area sA (m²/kg/s)	96.7909
Specific heat consumption sQ (kJ/Kg)	268.8019
Specific exergy consumption S_{ex} (kJ/Kg)	320.7198
Gain output ratio GOR	7.6235
Unit water cost ($/m³)	4.1712

change in the heat transfer areas. As it can be seen, both of the specific heat and exergy consumptions have higher values. It is because they are related to the mass flow rate and the temperature of the motive steam, which is supplied directly from the boiler and consequently higher motive steam pressure (and temperature) needed a higher energy. It can be reported from this table that the GOR value is 7.6235 while the actual value is 7.223. As the input motive steam flow rate to the unit is constant, the GOR value is directly related to the produced fresh water flow rate. The calculation results show that the production cost is 4.1712 $/m³ and less than the cost presents by the GCT factory which is 4.8 $/m³. This difference could be explained by the economic assumptions used in this model.

6.3. Parametric study

A parametric study was carried out and it is reported below for the SIDEM desalination unit to study the sensitivity analysis of the variation of; the motive steam mass flow rate, motive steam pressure and the feed seawater temperature to effects on the system's performance and the unit product cost.

6.3.1. Effect of motive steam flow rate:

The influence of the motive steam flow variation from 2 to 4 t/h on the total produced flow rate and the GOR values are shown in Fig. 7. The increase of the motive steam flow leads to 31% of produced flow rate increase and 34% of GOR decrease. Fig. 8 shows that the variation of the motive steam flow has a higher influence on the specific heat consumption and specific exergy consumption. That causes increase of 50% of specific heat consumption and 47% of
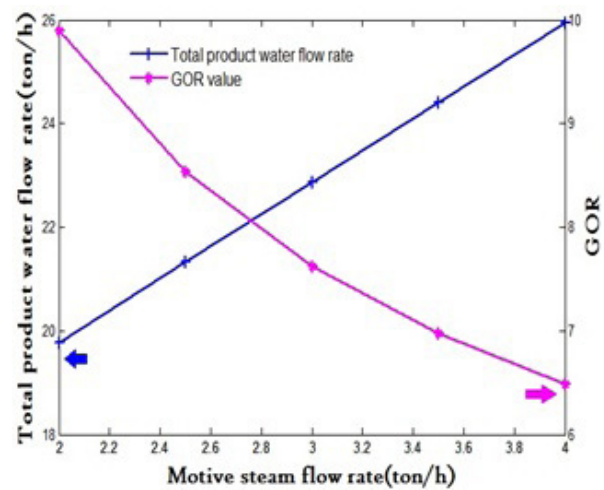
Fig. 7. Effect of motive steam flow rate on the total produced water flow rate and GOR.
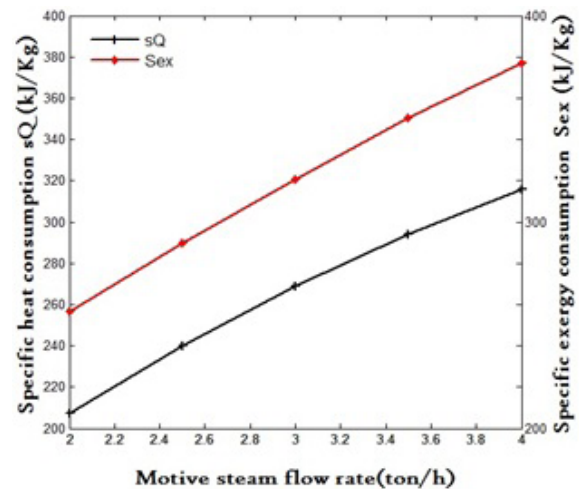
Fig. 8. Effect of motive steam flow rate on the specific heat consumption and specific exergy consumption.

the specific exergy consumption. The addition of steam flow rate leads to an increase in the temperature and the pressure of compressed vapor, which need a higher energy to evaporate the seawater in all effects. Furthermore, the motive steam flow variation shows a reduction in specific

heat transfer area of 12.42 % and an increasing of 11% in the salinity of rejected brine (from 55,400 to 61,500 ppm). Furthermore, in this case, the addition of the motive steam flow to the unit can decrement the produced water cost to 20.6% as indicated in Fig. 9.

6.3.2. Effect of motive steam pressure

The effect of the motive steam pressure variation on the total produced water and the GOR of the unit are presented in Fig. 10. An increase of the motive steam pressure from 1 to 7 bar leads to a reduction lower than 1% of both total produced water and the GOR values. Moreover, the increase of the motive steam pressure giving a slight variation on the specific heat and exergy consumptions as shown in Fig. 11. Fig. 12 shows that the increase of P_m leads to 5%increase of sA. As a results of P_m variation, the pressure of compressed vapor increases from 0.23 to 0.25 bars, the temperature of the compressed vapor is 8° C lower and the produced water cost increases is around 1.9% (4.12 to 4.2 $/m³).
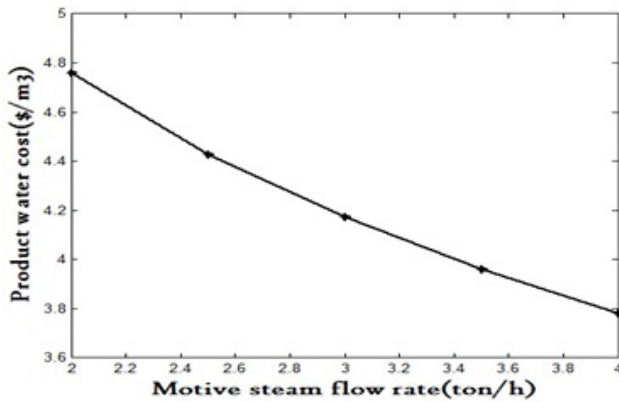
Fig. 9. Effect of motive steam flow rate on the unit produced water cost.
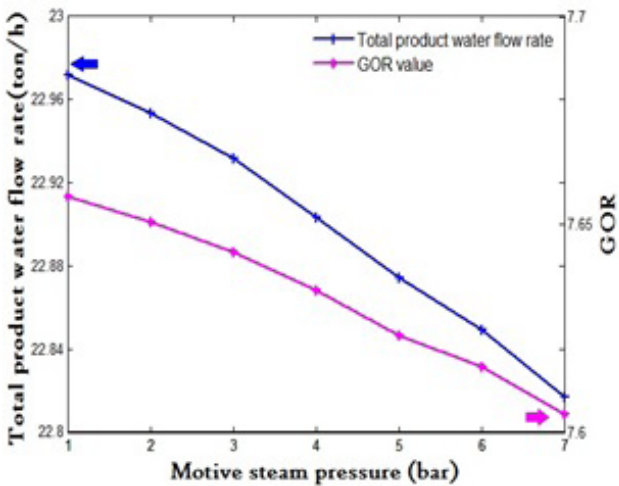
Fig. 10. Effect of motive steam pressure on the total produced water flow rate and GOR.

6.3.3. Effect of feed sea water temperature

The effect of the feed seawater to effects temperature variation on the produced water mass flow rate and the GOR value is shown in Fig. 13. The increase of the tem-
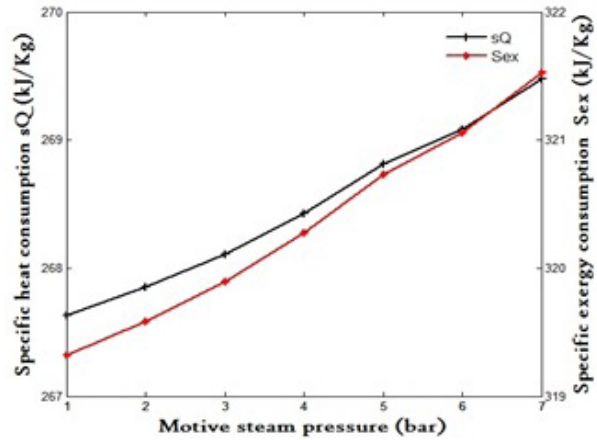
Fig. 11. Effect of motive steam pressure on the specific heat consumption and specific exergy consumption.
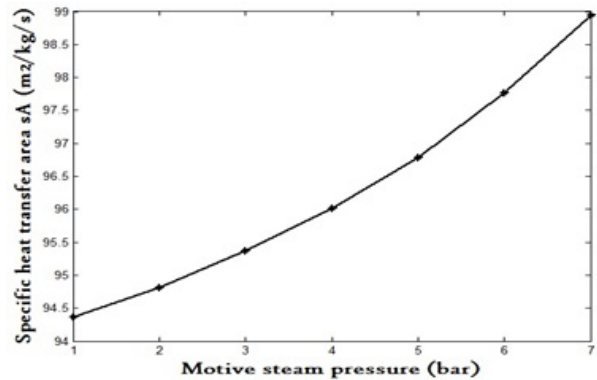
Fig. 12. Effect of motive steam pressure on the specific heat transfer area.
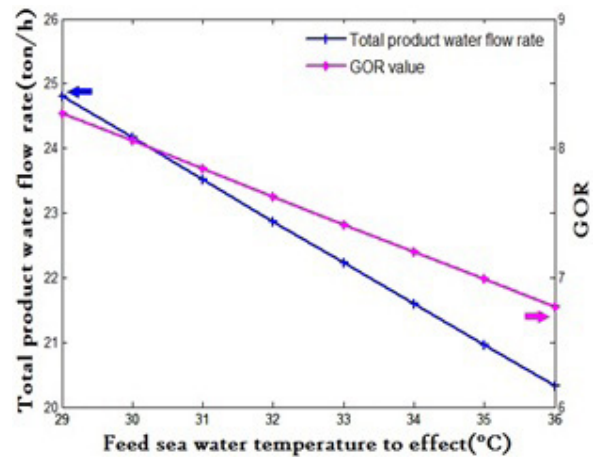
Fig. 13. Effect of feed seawater temperature on the total produced water flow rate and GOR.
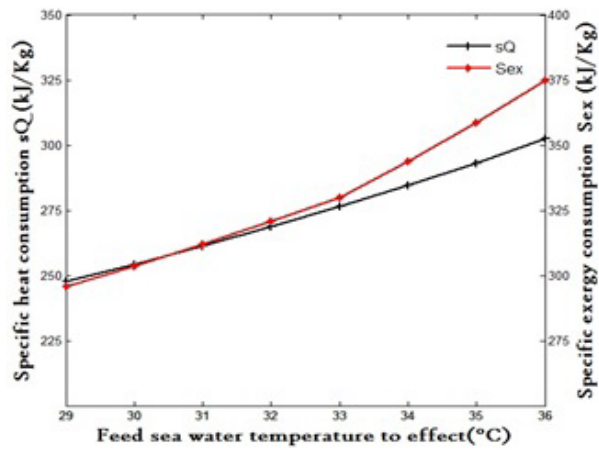
Fig. 14. Effect of feed seawater temperature on the specific heat consumption and specific exergy consumption.
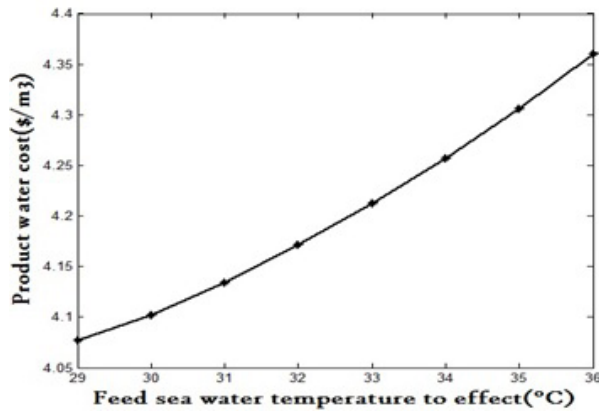
Fig. 15. Effect of feed sea water temperature on the unit product water cost.

perature from 29 to 36°C causes about 18% decrease in the produced water mass flow and the GOR. In addition, the temperature of compressed vapor (outlet the TVC) increases by 15°C which decreases the specific heat transfer area of the effects. As the mass flow rate of the feed seawater is constant, the temperature variation reduces the salinity of rejected brine from 61,300 to 54,800 ppm. As shown in Fig. 14, the two specific heat and exergy consumptions increase by 22% and 26%, respectively. The effect of increasing the feed temperature on the produced water cost of the unit is shown in Fig. 15. It causes the rise in the cost value with 7% (4.07 to 4.36 $/m³).

7. Conclusions

This paper presents a modeling and simulation of a MED-TVC desalination system located in the GCT factory in Tunisia. A mathematical and economic model was developed and used to minimize the total annual cost of the unit. This paper proposed a new connection between a process optimizer and process simulator is investigated to solve the problem. The configuration of problem was built with five decision variables and feasibility constraints as the salinity of rejected brine. Simulation results show a good agreement with the actual data from the factory. Moreover, parametric analyses of the SIDEM unit performance were established. The increase in motive steam flow rate causes about 20.6% reduction in the product cost. In addition, the increase of feed seawater temperature to effects causes about 7% rise in the cost. The increase in the pressures of motive steam and compressed vapor increase about 1% in the product cost.

Symbols

A	—	Heat transfer area, m²
B	—	Brine flow rate, ton/h
BPE	—	Boiling point elevation, °C
C_p	—	Specific heat capacity of water, kJ/kg °C
CR	—	Compression ratio
D	—	Mass flow rate of distillate, ton/h
F_{BM}	—	Correction factor for the capital cost
F	—	Feed seawater flow rate, ton/h
H	—	Specific enthalpy, kJ/kg
i_r	—	Factor of annualized capital cost
$LMTD$	—	Logarithmic mean temperature difference, °C
M	—	Mass flow rate, ton/h
M_B	—	Rejected Brine, ton/h
n	—	Number of effects, Last effect
NEA	—	Non-equilibrium allowance, °C
P	—	Pressure, kPa
ppm	—	Parts per million
Q_e	—	Heat flow in effect, kW
R_a	—	The entrainment ratio
S	—	Specific entropy, kJ/kg °C
s	—	Salinity, g/kg
sA	—	Specific heat transfer area, m²/kg/s
T	—	Temperature, °C
U	—	Overall heat transfer coefficient, kW/m² °C
V	—	Vapor mass flow rate, ton/h
X	—	Salt concentration, ppm
ΔT	—	Temperature difference between effects, °C

Greek

λ	—	Latent heat of evaporation, kJ/kg

Subscripts

b	—	Brine
c	—	Vapor to condenser
con	—	Condenser

cv	—	Compressed vapor
cw	—	Cooling seawater
d	—	Distillate product
e	—	effect
eq	—	Inequality
ev	—	Entrained vapor
evp	—	Evaporator
f	—	Feed seawater to effects
i : 1, 2, 3	—	Effect index
m	—	Motive steam
sw	—	Input seawater
t	—	total
v	—	Vapor formed from boiling
y	—	Year

References

[1] A. Seamonds, International Desalination Association (IDA): IDA Desalination Yearbook 2016-2017, USA: Topsfield, M.A., 2016. Available from: http://idadesal.org/wp-content/.

[2] H.T. El-Dessouky, H.M. Ettouney, Fundamentals of Salt Water Desalination, Elsevier, 2002.

[3] I.S. Al-Mutaz, I .Wazeer, Development of a steady-state mathematical model for MEE-TVC desalination plants, Desalination, 351 (2014) 9–18.

[4] A.O. Bin Amer, Second law and sensitivity analysis of large ME-TVC desalination units, Desal. Water Treat., 53 (2015) 1234–1245.

[5] J.H. Lienhard V, In: H.A. Arafat, Desalination Sustainability A Techincal, Socioeconomic, and Environmental Approach, Elsevier Publishing, 2017, pp. 127–206.

[6] H. Al-Fulaij, A. Cipollina, D. Bogle, H. Ettouney, Steady state and dynamic models of multistage flash desalination: A review, Desal. Water Treat., 13 (2010) 42–52.

[7] S.N. Malik, P.A. Bahri, L.T.T. Vu, Steady state optimization of design and operation of desalination systems using Aspen Custom Modeler, Comput. Chem. Eng., 91 (2016) 247–256.

[8] S. Azimibavil, A.J. Dehkordi, Dynamic simulation of a multi-effect distillation (MED) process, Desalination, 392 (2016) 91–101.

[9] M. Khamis Mansour, Hassan E.S. Fath, Numerical simulation of flashing process in MSF flash chamber, Desal. Water Treat., 51(10–12) (2013) 2231–2243.

[10] F. Alamolhodaa, R. KouhiKamalib, M. Asgari, Parametric simulation of MED–TVC units in operation, Desal. Water Treat., 57 (2015) 1–14.

[11] S.E. Shakib, M. Amidpour, C. Aghanajafi, A new approach for process optimization of a METVC desalination system, Desal. Water Treat., 37 (2012) 84–96.

[12] K.H. Mistry, M.A. Antar, J.H. Lienhard V, An improved model for multiple effect distillation, Desal. Water Treat., 51 (2013) 807–821.

[13] R. Kouhikamali, A. Samami Kojidi, M. Asgari, F. Alamolhoda, The effect of condensation and evaporation pressure drop on specific heat transfer surface area and energy consumption in MED–TVC plants, Desal. Water Treat., 46 (2012) 68–74.

[14] R. Kouhikamali, Z. FallahRamezani, M. Asgari, Investigation of thermo-hydraulic design aspects in optimization of MED plants, Desal. Water Treat., 51 (2013) 5501–5508.

[15] I.S. Al-Mutaz, I. Wazeer, Optimization of location of thermo-compressor suction in MED-TVC desalination plants, Desal. Water Treat., 57 (2016) 1–15.

[16] T.H. Dahdah, A. Mitsos, Structural optimization of seawater desalination: I. A flexible superstructure and novel MED–MSF configurations, Desalination, 344 (2014) 252–265.

[17] T.H. Dahdah, A. Mitsos, Structural optimization of seawater desalination: II novel MED–MSF–TVC configurations, Desalination, 344 (2014) 219–227.

[18] M. Skiborowski, A. Mhamdi, K. Kraemer, W. Marquardt, Model-based structural optimization of seawater desalination plants, Desalination, 292 (2012) 30–44.

[19] H. Sayyaadi, A. Saffari, Thermoeconomic optimization of multi effect distillation desalination systems, Appl. Energy, 87 (2010) 1122–1133.

[20] A. Piacentino, Application of advanced thermodynamics, thermoeconomics and exergy costing to a multiple effect distillation plant: In-depth analysis of cost formation process, Desalination, 371 (2015) 88–103.

[21] M.S. Tanvir, I.M. Mujtaba, Optimisation of design and operation of MSF desalination process using MINLP technique in gPROMS, Desalination, 222 (2008) 419–430.

[22] P. Druetta, P. Aguirre, S. Mussati, Minimizing the total cost of multi effect evaporation systems for seawater desalination, Desalination, 344 (2014) 431–445.

[23] I.J. Esfahani, A. Ataei, V.K. Shetty, T. Oh, J.H. Park, C. Yoo, Modeling and genetic algorithm-based multi-objective optimization of the MED-TVC desalination system, Desalination, 292 (2012) 87–104.

[24] M.H. Khademi, M.R. Rahimpour, A. Jahanmiri, Simulation and optimization of a six-effect evaporator in a desalination process, Chem. Eng. Process.: Process Intensif., 48 (2009) 339–347.

[25] M.A. Darwish, A.A. El-Hadik, The multi-effect boiling desalting system and its comparison with the multi-stage flash system, Desalination, 60 (1986) 251–265.

[26] R.B. Power, Steam Jet Ejectors for the Process Industries, McGraw-Hill, New York, 1994.

[27] A.K. Coker, Ludwig's Applied Process Design for Chemical and Petrochemical Plants, Fourth Edition, Elsevier, USA, 2007.

[28] R. Turton, R.C. Bailie, W.B. Whiting, Analysis, Synthesis, and Design of Chemical Processes, 4thed., Prentice Hall, New York, NY, 2012.

[29] S. Al-Hengaria, W. ElMoudira, M.A. El-Bousiffi, Economic assessment of thermal desalination processes, Desal. Water Treat., 55 (2015) 2423–2436.

[30] Y. Zhou, R.S.J. Tol, Evaluating the costs of desalination and water transport, Water Resour. Res., 41 (2005) W03003:1–10.

[31] V.C. Onishi, A. Carrero-Parreño, J.A. Reyes-Labarta, R. Ruiz-Femenia, R. Salcedo-Díaz, E.S. Fraga et al., Shale gas flowback water desalination: Single vs multiple-effect evaporation with vapor recompression cycle and thermal integration, Desalination, 404 (2017) 230–248.

[32] J.R. Couper, W.C. Penney, J.R. Fair, S.M. Walas, Chemical process equipment, selection and desing, 2nd ed., Elsevier, USA, 2010.

[33] Optimization Toolbox User's Guide, the Math Works, Available online: http://www.mathworks.com, 2017.

[34] A. Messac, Optimization in Practice with MATLAB for Engineering Students and Professionals, Cambridge University Press, USA, 2015.

[35] A.O. Bin Amer, Development and optimization of ME-TVC desalination system, Desalination, 294 (2009) 1315–1331.

[36] E. Gencer, R. Agrawal, Strategy to synthesize integrated solar energy coproduction processes with optimal process intensification. Case study: Efficient solar thermal hydrogen production, Comput. Chem. Eng., 105 (2017) 328–347.

[37] M.A. Navarro-Amoros, R. Ruiz-Femenia, J.A. Cabellero, Integration of modular process simulators under the generalized disjunctive programming framework for the structural flowsheet optimization, Comput. Chem. Eng., 67 (2014) 13–25.

[38] Y. Li, X. Huang, H. Peng, X. Ling, S. Tu, Simulation and optimization of humidification-dehumidification evaporation system, Energy, 145 (2018) 128–140.

[39] H.T. El-Dessouky, H.M. Ettouney, F. Mandani, Performance of parallel feed multiple effect evaporation system for seawater desalination, Appl. Therm. Eng., 20 (2000) 1679–1706.

[40] M.T. Mazini, A. Yazdizadeh, M.H. Ramezani, Dynamic modeling of multi-effect desalination with thermal vapor compressor plant, Desalination, 353 (2014) 98–108.

Appendix

Thermodynamics properties of Seawater [2,39,40]

The thermodynamics properties of seawater are equations depends on temperature T and salinity X, they are as below:

The seawater specific heat capacity C_p:

$$C_p = \left[A + BT + CT^2 + DT^3 \right] \times 10^{-3} \qquad (A.1)$$

The variables A, B, C and D are a function of the water salinity as follows:

$$A = 4206.8 - 6.6197s + 1.2288 \times 10^{-2} s^2 \qquad (A.2)$$

$$B = -1.1262 + 5.4178 \times 10^{-2} s - 2.2719 \times 10^{-4} s^2 \qquad (A.3)$$

$$C = 1.2026 \times 10^{-2} - 5.3566 \times 10^{-4} s + 1.8906 \times 10^{-6} s^2 \qquad (A.4)$$

$$D = 6.8777 \times 10^{-7} + 1.517 \times 10^{-6} s - 4.4268 \times 10^{-9} s^2 \qquad (A.5)$$

where C_p in kJ/(kg°C), T in °C and s in g/kg . This correlation is valid over the salinity and temperature ranges of $20{,}000 \le X \le 160{,}000$ ppm and $20 \le T \le 180°C$, respectively.

The boiling point elevation (BPE):

$$BPE = X\left(B + CX\right)10^{-3} \qquad (A.6)$$

with the variables B and C are a function of temperature as follows:

$$B = \left(6.71 + 6.34 \times 10^{-2} T + 9.74 \times 10^{-5} T^2\right)10^{-3} \qquad (A.7)$$

$$C = \left(22.238 + 9.59 \times 10^{-3} T + 9.42 \times 10^{-5} T^2\right)10^{-8} \qquad (A.8)$$

where BPE and T in °C and X in ppm.

The latent heat of vaporization λ

$$\lambda = 2501.897149 - 2.407064037T + 1.192217 \times 10^{-3} T^2 - 1.5863 \times 10^{-5} T^3 \qquad (A.9)$$

where λ in kJ/kg and T in °C.

The specific enthalpy of saturated liquid water h_l:

$$h_l = -0.033635409 + 4.20755011T - 6.200339 \times 10^{-4} T^2 + 4.459374 \times 10^{-6} T^3 \qquad (A.10)$$

where h_l in kJ/kg and T in °C.

The specific enthalpy of saturated vapor water h_v:

$$h_v = 2501.689845 + 1.806916015T + 5.087717 \times 10^{-4} T^2 - 1.1221 \times 10^{-5} T^3 \qquad (A.11)$$

where h_v in kJ/kg and T in °C.

The specific entropy of saturated liquid water S_l:

$$S_l = -0.00057846 + 0.015297489T - 2.63129 \times 10^{-5} T^2 + 4.11959 \times 10^{-8} T^3 \qquad (A.12)$$

where S_l in kJ/(kg°C) and T in °C.

The specific entropy of saturated vapor water S_v:

$$S_v = 9.149505306 - 2.581012 \times 10^{-2} T + 9.625687 \times 10^{-5} T^2 - 1.786615 \times 10^{-7} T^3 \qquad (A.13)$$

where S_v in kJ/(kg°C) and T in °C.